Proceedings of the XVII ECSMGE-2019
Geotechnical Engineering foundation of the future
ISBN 978-9935-9436-1-3

doi: 10.32075/17ECSMGE-2019-0346

XVII European Conference
ECSMGE 2019
Reykjavik
on Soil Mechanics
and Geotechnical Engineering

Modelling rainfall-induced landslides with the material point method: the Fei Tsui Road case

Modélisation des glissements de terrain induits par les précipitations avec la méthode des points matériels: le cas de la route Fei Tsui

Wei-Lin LEE
Department of Hydraulic and Ocean Engineering, National Cheng-Kung University, Tainan, Taiwan (R.O.C.)

Mario Martinelli
Deltares, Delft, The Netherlands

Chjeng-Lun SHIEH
Department of Hydraulic and Ocean Engineering, National Cheng-Kung University, Tainan, Taiwan (R.O.C.)

ABSTRACT: Rainfall-induced landslides seriously affect the safety of residents and properties in the surrounding area. In particular, landslides exhibit large mobilized volume with very large displacement. For this reason, the numerical modeling of a landslide is a challenging problem, as it requires a good pre-failure and post-failure description after large deformations process. For this reason, a dynamic fully coupled model using material point method is proposed to describe the landslide failure problem from the triggering phase until the complete runout. The Fei Tsui Road landslide in Hong Kong is used as a case study for the validation of this numerical tool.

RÉSUMÉ: Les glissements de terrain provoqués par les précipitations compromettent gravement la sécurité des habitants et des propriétés des environs. En particulier, les glissements de terrain entraînent des volumes mobilisés importants avec des déplacements très importants. Pour cette raison, la modélisation numérique du glissement de terrain est un problème complexe, car elle nécessite une bonne description avant et après la défaillance après un processus de déformations importantes. Pour cette raison, un modèle entièrement couplé dynamique utilisant la méthode des points matériels est proposé pour décrire le problème d'échec de glissement de terrain depuis la phase de déclenchement jusqu'à l'arrivée complète. Le glissement de terrain de la route Fei Tsui à Hong Kong est utilisé comme étude de cas pour la validation de cet outil numérique.

Keywords: landslide, material point method, large deformation, unsaturated soil;

1 INTRODUCTION

On 12-13 August 1995, a landslide occurred at Fei Tsui Road in Chai Wan, Hong Kong (HK), during intense rainfall related to the passing of a typhoon (Knii 1996). The Fei Tsui Road landslide, with a volume of about 14000 m3, is one of the largest slope failures reported in Hong Kong over the last few decades. A picture of the disaster is shown in Figure 1. Some researchers tried to simulate the failure process

of the landslide. Chen and Lee (2000) adopted the Lagrangian Galerkin finite element method to simulate only the propagation stage. Wang and Sassa (2010) used field observations to validate the accuracy of their model, which is based on depth-integrating Navier–Stokes equations and an apparent friction varying during the landslide motion. Sanchez et al. (2013) compared the field measurements after the Fei Tsui Road landslide with the results of their landslide propagation modeling conducted by means of SPH method. Cuomo et al. (2015, 2017) and Calvello et al. (2017) combined SPH and inverse analysis to propagation analysis and for rheology calibration of the Fei Tsui Road Landslide. Then, Cuomo et al. (2019) studied the role of soil cohesion on the propagation features using simplified MPM analyses. These previous studies were more focused on the propagation phase, wherease, the present paper investigates the complete failure process –from the triggering phase to the complete runout - using the material point method (MPM).

Figure 1 The Fei Tsui Road landslide on 13th Aug. in 1995 (Knill, 2006)

MPM is a mesh-free method, originally developed by Sulsky et al. (1994) to simulate large deformations process in single-phase materials. This approach avoids mesh distortion by combining the advantages of Lagrangian and Eulerian method, and so large deformation problems with history-dependent materials can be simulated. Many researchers extended this method to simulate coupled hydro-mechanical problems in porous media (Zabala and Alonso 2011; Kafaji 2013; Jasmin et al., 2013, Abe et al. 2013). Some researchers also used MPM to investigate the entire failure process or rainfall induced landslides. In particular, Yerro et al. (2015) developed a full 3-phase formulation where the gas velocity is one of the primary unknowns of the system. Wang et al. (2018) proposed a simplified version of 3-phase formulation, where suction and saturation are taken into account but the variation of gas pressure is assumed to be negligible.

In this study, the formulation proposed by Wang et al. (2018) and described in the following was implemented to simulate the Fei Tsui Road landslide.

2 MPM FORMULATION FOR UNSATURATED SOIL

The set if equations of the dynamic formulation are described in this section, where the primary unknowns are the velocities of soil and water, indicated by the superscripts of w and s respectively (v^s-v^w formulation) (Jassim et al, 2013)

2.1 Conservation of mass

The conservation of soil mass is written as follows

$$\frac{dn}{dt} = (1-n)\nabla \cdot \boldsymbol{v}^s , \tag{1}$$

where 1-n is the volume fraction of soil phase over the total volume and n is the porosity, ρ^s is the true densities of soil phase, t is the time, and $\boldsymbol{v}^s$ is the velocities of soil phase. This equation is derived assuming that the gradient of porosity is negligible and the solid particles are incompressible.

The conservation of water mass is described as

$$nS^w \frac{\partial \rho^w}{\partial t} + n\rho^w \frac{\partial S^w}{\partial t} + S^w \rho^w (1-n) \nabla \cdot \boldsymbol{v}^s n S^w \rho^w \nabla \cdot \boldsymbol{v}^w = 0 \quad , \tag{2}$$

where S^w is the degree of saturation, ρ^w is the true density of water phase, and $\boldsymbol{v}^w$ is the velocity of water phase. This equation is derived assuming that the gradient of porosity is negligible.

Assuming a weakly-compressible fluid, the pore water pressure (p^w) can be computed as follows:

$$-\frac{1}{\rho^w}\frac{\partial \rho^w}{\partial t} = \frac{1}{K^w}\frac{\partial p^w}{\partial t}, \tag{3}$$

where K^w is the bulk modulus of water phase. In unsaturated soils, the pore water can be trapped in the soil pores by the suction (p^c = -(p^a - p^w)), which is a positive pore water pressure above a phreatic surface, where p^a is pore air pressure. By using the chain rule of differentiation, and assuming that there is no variation in time of the air pressure, the time derivative of the saturation is derived as

$$\frac{\partial S^w}{\partial t} = \frac{\partial S^w}{\partial p^c}\frac{\partial p^c}{\partial t} = \frac{\partial S^w}{\partial p^c}\frac{\partial p^w}{\partial t} . \tag{4}$$

By substituting equations of (3) and (4) into equation (2), the conservation of water mass can be obtained as

$$\frac{\partial p^w}{\partial t} = \lambda \left[(1-n) \nabla \cdot \boldsymbol{v}^s + n \nabla \cdot \boldsymbol{v}^w \right], \tag{5}$$

where $\lambda = \left(\frac{n}{K^w} - \frac{n}{S^w}\frac{\partial S^w}{\partial p^c} \right)^{-1}$.

2.2 Conservation of momentum

The conservation of momentum is imposed for the water and the mixture. The momentum equation for water is:

$$\rho^w \boldsymbol{a}^w = \nabla p^w + \rho^w \mathbf{b} - \frac{n S^w \mu^w}{k\ K^w_{rel}} \left(\boldsymbol{v}^w - \boldsymbol{v}^s \right), \tag{6}$$

where $\boldsymbol{a}^w$ is the acceleration of the water, $\mathbf{b}$ is the body force vector, μ^w is the dynamic viscosity of the water, and k as well as K^w_{rel} are respectively the intrinsic permeability and relative permeability of the solid skeleton. The relative permeability is the ratio between the current soil permeability (with a given degree of saturation) and the one in fully saturated condition.

The conservation of momentum of mixture is:

$$(1-n)\rho^s \boldsymbol{a}^s + n S^w \rho^w \boldsymbol{a}^w = \nabla \cdot \boldsymbol{\sigma} + \left[(1-n)\rho^s + n S^w \rho^w \right] \mathbf{b}, \tag{7}$$

where $\boldsymbol{a}^s$ is the acceleration of the soil phase, and $\boldsymbol{\sigma}$ is the total stress of the mixture. Bishop's effective stress (Bishop, 1954) is utilized by assuming that the effect of pore air pressure change is neglected, it can be described by

$$\boldsymbol{\sigma} = \boldsymbol{\sigma}' + \chi p_w \mathbf{I}, \tag{8}$$

where $\boldsymbol{\sigma}'$ is the effective stress vector, $\mathbf{I}$ is the unit vector, and χ is an effective stress parameter called matrix suction coefficient. In this paper, χ is set to the degree of saturation S^w.

2.3 Hydraulic constitutive equation

The van Genuchten (1980) equation is used to describe the relationship between the degree of saturation and suction, as follows

$$S^w(p^c) = S^w_r + \left(S^w_s - S^w_r \right) \left[1 + \left(\frac{p^c}{\alpha} \right)^{\frac{1}{1-\beta}} \right]^{-\beta}, \tag{9}$$

where β is empirical coefficient, and α is called air entry value.

The relative permeability is expressed as a function of degree of saturation according to Mualem (1976), as follows

$$k^w_{rel}\left(S^w\right) = \left(S_e\right)^{0.5} \left[1 - \left(1 - S_e^{\frac{1}{\beta}} \right)^{\beta} \right]^2 . \tag{10}$$

with S_e as the effective saturation, defined as

$$S_e = \frac{S^w - S^w_r}{S^w_s - S^w_r} . \tag{11}$$

where S^w is the current degree of saturation, and S^w_r and S^w_s are respectively the degrees of saturation at full saturation and at very dry condition respectively.

2.4 Algorithm of Material point method

A schematic representation of the material point method and the background mesh is shown in Figure 2. The points represent the material discretization and the background mesh is used for the computational step.

In this formulation, each material point carries information of the solid and liquid constituent, like mass, momentum, effective stress and liquid pressure. The background mesh is only used to solve the $\boldsymbol{v}^s$-$\boldsymbol{v}^w$ formulation at the nodes and map information to particles.

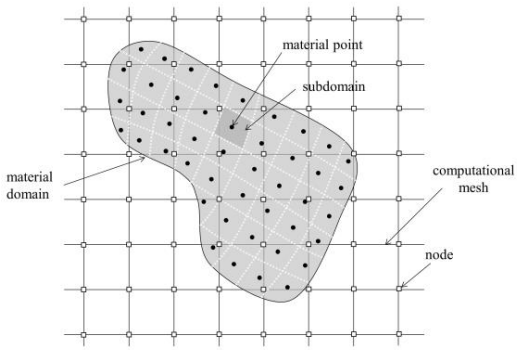

Figure 2 Spatial discretization in MPM (Yerro, 2015)

A single computational cycle is described as follows:

(a).$\boldsymbol{a}^w$ is solved on the node by the discretized form of eq. (6)

(b). $\boldsymbol{a}^w$ is substituted into the discretized form of eq. (7) and $\boldsymbol{a}^s$ is obtained.

(c). The material point velocities are computed from the nodal accelerations.

(d). The nodal velocities are computed as the ratio between nodal momentum and nodal mass.

(e). Strain increment are then computed at the location of each material point.

(f). The increments of pore water pressure and effective stress are solved by equations (5) and (8), respectively.

(g). Displacement and position of each material point is updated.

The explicit integration scheme, such as the one presented above, is conditionally stable. The size of the timestep for stable solution depends on the properties of the materials: it decreases with stiffness and with low permeability.

3 THE FEI TSUI ROAD LANDSLIDE

A rainfall event of 55 hours, starting from 00:00 AM of the 11th Aug. 1995, occurred in Hong Kong and a large landslide was triggered. The histogram of rainfall event is shown in Figure 3, where the rainfall intensity increases progressively reaching the maximum value of 66 mm/hr (which corresponds to 1.83 10^{-5} m/s).

According to the report from Knill (2006), the first slope failure occurred at 00:55 AM on the 13th Aug. 1995 (after 49 hours of rainfall in Figure 3) with a volume of landslide of about 10 m^3. The major failure was triggered at 01:15 AM, with a volume of about 14000 m^3, and the distance of runout was approximately 30 meters. The pre-failure and post-failure topography are shown in Figure 4, together with the geological settings.

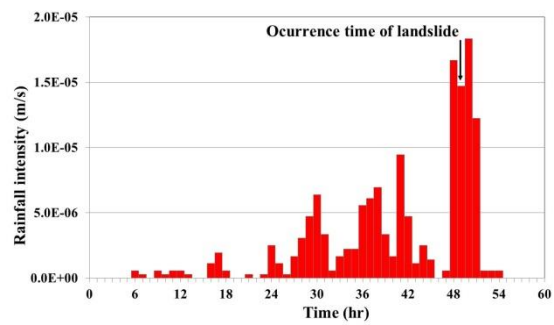

Figure 3 Histogram of rainfall recording (Knill, 2006)

Before failure, the dip of the slope was approximately 62°. The stratigraphy is composed of a weathered volcanic rock of about 22m thick, overlaying an altered tuff layer of about 3m thick. The weathered rock consists of a completely to slightly decomposed tuff. The

upper part of the slope is a fresh volcanic rock that becomes visible after the failure of a slope (Figure 1), with an inclination of the surface of approximately 52°.

After failure, a comprehensive set of geotechnical laboratory tests was conducted on soil samples during the ground investigation (Knill, 2006) to identify the main soil properties of the weathered volcanic rock and the alterated tuff. On average, the friction angle of the weathered volcanic rock is 35° and cohesion is zero. Conversely, the average friction angle of the altered tuff layer is 22° and the cohesion is zero. For both soils, the saturated unit weight is about 19 kN/m^3 and the range of saturated hydraulic conductivity is between 10^{-5} m/s and 10^{-7} m/s.

Based on the available information from Knill (2006), it was assumed that two groundwater regimes existed at the site at the time of the landslide: a regional groundwater table within the rock mass below the altered tuff layer, and a perched water table in the weathered volcanic soil overlying the altered tuff layer.

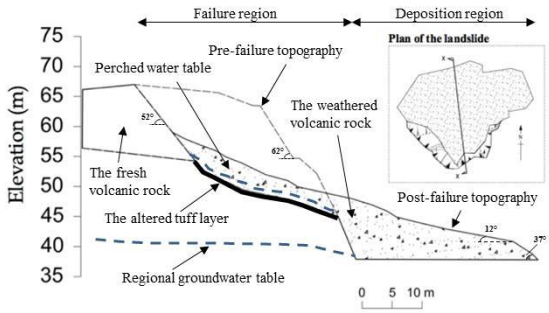

Figure 4 The topography of the Fei Tsui Road landslide (Knill, 2006)

4 THE NUMERICAL MODEL

In this present study, the Fei Tsui Road landslide is simulated under plane-strain condition using a cross section shown in Figure 4. The computational domain with different properties is shown in Figure 5. A total of 25011 triangular elements with mesh size of about 1 meter are assigned uniformly in the computational domain. The material points representing the base are fixed in space and are used to define the contact surfaces. Two contact properties are defined along the contact surface. The contact friction angle along *contact surface A* is set to 22° (equal to the internal friction of the altered tuff layer), whereas the contact friction angle along *contact surface B* is 35°.

The stress-strain response of the weathered and the fresh volcanic rock is modelled as an elasto-plastic material with a failure criterion defined by Mohr-Coulomb.

The unsaturated characteristics of the materials are not mentioned in the GEO report, and so these parameters are derived from different sources. Weathered volcanic tuff and weathered granite are two common soils in Hong Kong. Gan and Fredlund (1996), Wang and Yan (2006), Ng and Leung (2007), and Ng et al. (2011) performed several laboratory tests on these materials and they derived similar water-retention and hydraulic conductivity characteristic curves. The curves used in this paper are shown in Figure 6. The hydraulic conductivity is assumed as the maximum value ($k=10^{-5}m/s$) of the interval proposed by Knill (2006). The complete list of all parameters is shown in Table 1.

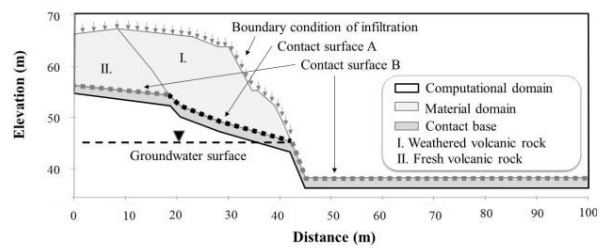

Figure 5 Summary of geometry and material domains for the Fei Tsui Road landslide.

Because the numerical scheme is explicit, the calculation is conditionally stable and the timestep increments are very small. For this reason, the permeability is set to $5{\cdot}10^{-3}$m/s (500 times larger than the real one) and it is kept

constant during the simulation (K_{rel}^{w} set to 1). The bulk modulus of water is also decreased by a factor of 100.

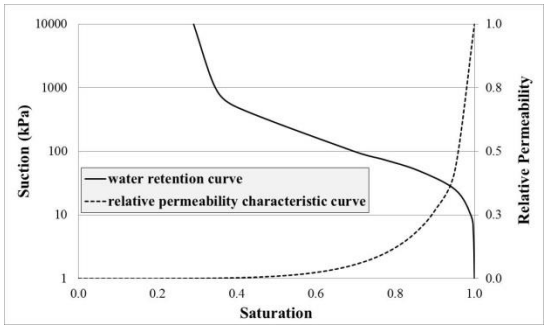

Figure 6 The water retention curve (black line) and the relative permeability characteristic curve (black dash line) of the weather volcanic rock.

Table 1 Material parameters for slope analysis.

parameters	units	values
S_r^w	-	0.28
S_s^w	-	1
α	kPa	65.789
β	-	0.47
k	m^2	10^{-12}
K_w	kPa	20000
μ^w	Pa·s	10^{-6}
n	-	0.45
ρ_s	kg/m^3	2650
ρ_w	kg/m^3	1000
E	kPa	50000
ν	-	0.3
c	kN/m^2	0 (I-weathered); 50 (II-intact)
ϕ	°	35
ϕ'	°	22 (Contact surf A); 35 (Contact surf B)

5 THE PROCESS OF RAINFALL-INDUCED LANDSLIDE

The numerical simulation has two steps: stress initialization and failure process induced by the rainfall event.

The initial distribution of pore water pressure is set as hydrostatic, based on the position of groundwater surface located at the toe of the slope. The suction above phreatic surface is also initialized. The suction plays an important role in the initial stability of the slope, as the dip of slope is very steep (approx. 62°).

The failure process is triggered by the rainfall event (Figure 3) with an intensity larger than the hydraulic conductivity. For this reason, the boundary condition for infiltration is modelled as ponding rainfall. It follows that, after equilibrium, a zero pore water pressure is applied to the slope surface (and consistently saturation becomes 1) to model continuous water infiltration into the slope.

Figure 7 and Figure 8 shows the failure of the slope when subjected to the rainfall infiltration, and the degree of saturation contours and the cumulative deviatoric strain are shown at four different time instants.

The beginning of failure occurs at the toe of slope where the degree of saturation is initially close to 1, and the suction in soil is low (*t=65s*). The increasing pore water pressure results in a decrease in soil strength, and so lateral support from downslope decreases. The wetting front infiltrates deeper into the soil body and a retrogressive failure is taking place (*t=150s*). Failure occurs progressively in part of the weathered rock close to the surface where the infiltration boundary condition is applied.

At time *t=220s*, the degree of saturation in the upper part of the slope is globally above 0.8, and a larger failure mechanism takes also place along the interface between weathered and intact rock.

Despite the fact that the values of permeability used in this calculation are extremely large compared to the measured values, the final configuration of the slope and the runout distance (*t=290s*) are in good agreement with the field observations after the disaster. The effect of the permeability on the final runout distance will be investigated in future study.

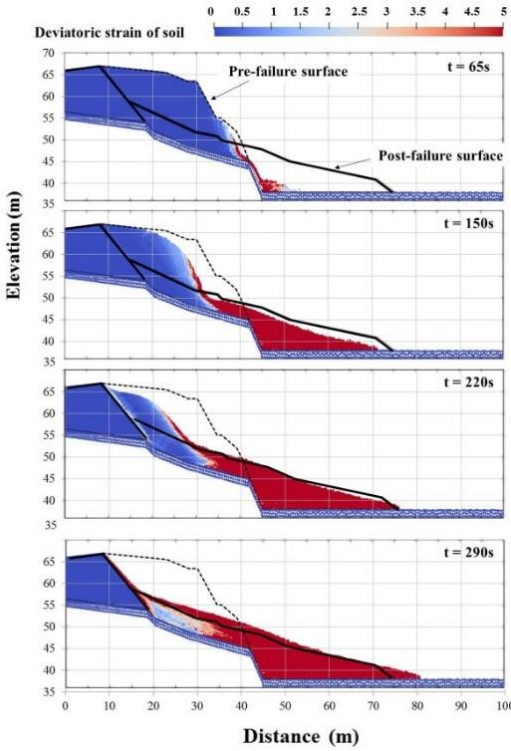

Figure 7 Evolution of deviatoric strain of soil during landslide process

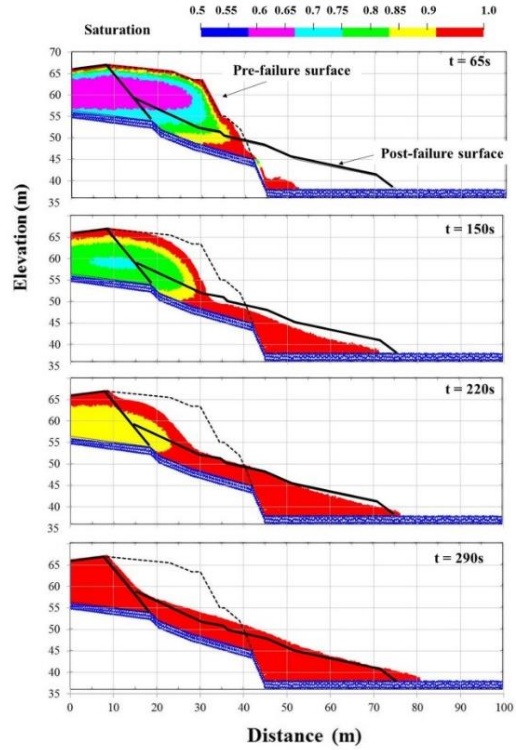

Figure 8 Evolution of the saturation during landslide process

6 CONCLUSION

This paper presents a dynamic fully coupled formulation to simulate rainfall-induced landslides with the material point method. This formulation is used to simulate the slope failure from the triggering phase until the complete runout. The Fei Tsui Road landslide in Hong Kong is used as a validation case study for this numerical tool. The numerical results show the evolution of unsaturated flow together with the slope deformations during the failure process, and they are in good agreement against the field observation after disaster. This method can be then utilized to investigate a wide range of slopes at risk of rainfall induce failure.

7 ACKNOWLEDGEMENTS

The authors would like to acknowledge Pooyan Ghasemi for his technical support during the set up of the case study.

8 REFERENCES

Abe, K., Soga, K., & Bandara, S. (2013). *Material point method for coupled hydromechanical prob-lems*. Journal of Geotechnical and Geoenvironmental Engineering, 140(3), 04013033.

Bishop, A. W. (1954). *The use of pore-pressure coefficients in practice*. Geotechnique, 4(4), 148-152.

Chen, H., & Lee, C. F. (2000). *Numerical simulation of debris flows*. Canadian Geotechnical Journal, 37(1), 146-160.

Calvello, M., Cuomo, S., & Ghasemi, P. (2017). *The role of observations in the inverse analysis of landslide propagation*. Computers and Geotechnics, 92, 11-21.

Cuomo, S., Calvello, M., & Villari, V. (2015). *Inverse analysis for rheology calibration in SPH analysis of landslide run-out*. In Engineering Geology for Society and Territory-Volume 2 (pp. 1635-1639). Springer, Cham.

Cuomo, S., Calvello, M., & Ghasemi, P. (2017). *Propagation modeling and inverse analysis of a landslide in Hong Kong*. In Workshop on World Landslide Forum (pp. 513-521). Springer, Cham.

Cuomo, S., Di Perna, A., Ghasemi, P., Martinelli, M., & Calvello, M., (2019). *Combined LEM and MPM analyses for the simulation of a fast moving landslide in Hong Kong*. II Int. Conf. On The Material Point Method For Modelling Soil–Water–Structure Interaction – Cambridge, UK.

Gan, J. K., & Fredlund, D. G. (1996). *Shear strength characteristics of two saprolitic soils*. Canadian Geotechnical Journal, 33(4), 595-609

Jassim, I., Stolle, D., & Vermeer, P. (2013). *Two‐phase dynamic analysis by material point method*. International journal for numerical and analytical methods in geomechanics, 37(15), 2502-2522.

Kafaji, I. K. A. (2013). *Formulation of a dynamic material point method (MPM) for geomechanical problems*.

Knill, S. J. (1996). *Report on the Fei Tsui road landslide of 13 August 1995*. Government Printer, South Africa.

Mualem, Y. (1976). *A new model for predicting the hydraulic conductivity of unsaturated porous media*. Water resources research, 12(3), 513-522.

Ng, C. W., & Leung, E. H. (2007). *Determination of shear-wave velocities and shear moduli of com-pletely decomposed tuff*. Journal of geotechnical and geoenvironmental engineering, 133(6), 630-640.

Ng, C. W. W., Wong, H. N., Tse, Y. M., Pappin, J. W., Sun, H. W., Millis, S. W., & Leung, A. K. (2011). *A field study of stress-dependent soil-water characteristic curves and permeability of a saprolitic slope in Hong Kong*. Géotechnique, 61(6), 511.

Sanchez, M. E., Pastor, M., & Romana, M. G. (2013). *Modelling of short runout propagation landslides and debris flows*. Georisk: Assessment and Management of Risk for Engineered Systems and Geo-hazards, 7(4), 250-266.

Sulsky, D., Chen, Z., & Schreyer, H. L. (1994). *A particle method for history-dependent materials*. Computer methods in applied mechanics and engineering, 118(1-2), 179-196.

Van Genuchten, M. T. (1980). *A closed-form equation for predicting the hydraulic conductivity of un-saturated soils 1*. Soil science society of America journal, 44(5), 892-898.

Wang, B., Vardon, P. J., & Hicks, M. A. (2018). *Rainfall-induced slope collapse with coupled material point method*. Engineering Geology, 239, 1-12.

Wang, F., & Sassa, K. (2010). *Landslide simulation by a geotechnical model combined with a model for apparent friction change*. Physics and Chemistry of the Earth, Parts A/B/C, 35(3), 149-161.

Wang, Y. H., & Yan, W. M. (2006). *Laboratory studies of two common saprolitic soils in Hong Kong*. Journal of geotechnical and geoenvironmental engineering, 132(7), 923-930.

Yerro Colom, A., Alonso Pérez de Agreda, E., & Pinyol Puigmartí, N. M. (2015). *The material point method for unsaturated soils*. Géotechnique, 65(3), 201-217.

Zabala, F., & Alonso, E. E. (2011). *Progressive failure of Aznalcóllar dam using the material point method*. Géotechnique, 61(9), 795-808.